Virology 527 (2019) 12–20

Contents lists available at ScienceDirect

Virology

journal homepage: www.elsevier.com/locate/virology

Bombyx mori nucleopolyhedrovirus protein Bm11 is involved in occlusion body production and occlusion-derived virus embedding

Haiping Wang, Weifan Xu, Xiangshuo Kong, Ying Fan, Xiaofeng Wu*

College of Animal Science, Zhejiang University, Hangzhou 310058, China

ARTICLE INFO

Keywords:
Baculovirus
BmNPV
Bm11
Subcellular localization
OB production
ODV occlusion

ABSTRACT

Bombyx mori nucleopolyhedrovirus (BmNPV) *orf11* (*bm11*) is a highly conserved gene with unknown function. It is homologous to AcMNPV *orf19*. In this study, a *bm11* knockout virus was constructed and its role was investigated. Expression analysis indicated that *bm11* is a late gene and confocal microscopy analysis demonstrated that Bm11 localizes predominantly in the nuclear ring zone at the late phase of infection. The *bm11* deletion did not affect budded virus (BV) production or viral genome replication, but markedly reduced the production of occlusion bodies (OBs) and the embedding of occlusion-derived viruses (ODVs). Bio-assays showed that Bm11 was involved in BmNPV infectivity *in vivo* by direct injection. In conclusion, our results demonstrated that although Bm11 is not essential for BV production or mature ODV formation, it affects OB production and ODV occlusion.

1. Introduction

Baculoviruses are a unique group of insect-specific viruses with double-stranded, circular, supercoiled genomes packaged into rod-shaped nucleocapsids enclosed by lipid envelopes (Herniou et al., 2003; Rohrmann, 2014). During the biphasic life cycle, baculoviruses produce two virion phenotypes, the budded virus (BV) and the occlusion-derived virus (ODV) (van Oers and Vlak, 2007), which have their nucleocapsid structure and genetic information in common, but differ in the origin of their envelopes (Braunagel and Summers, 1994; Slack and Arif, 2006). In addition, BVs mediate cell-to-cell infection inside the individual host, whereas ODVs initiate infection in the midgut epithelium and facilitate oral infection of the host (Granados and Lawler, 1981; Keddie et al., 1989). During the very late stage of infection, ODVs are formed from nucleocapsids retained in the nucleus, where they acquire envelopes from intranuclear microvesicles (Braunagel and Summers, 2007). The mature ODVs are then embedded within a protein matrix to form occlusion bodies (OBs). The structure of OBs physically protects the virions against detrimental influences in the environment. In the final phase of infection, OBs are liberated into the environment upon infected larvae liquefaction (Granados and Lawler, 1981; Keddie et al., 1989; Rohrmann, 2014), enabling ODVs to initiate primary infection of another susceptible host (Federici, 1997; Williams and Faulkner, 1997). Therefore, the occluded virions play an essential role in the infection of midgut cells.

As a typical species of *Alphabaculovirus* in the *Baculoviridae, Bombyx mori* nucleopolyhedrovirus (BmNPV) is a major pathogen of the silkworm, and often causes serious damage to the silk industry (Miao et al., 2005). BmNPV has a genome of approximately 128 kbp, which consists of 143 predicted open reading frames (ORFs) (Katsuma et al., 2011). Several ORFs are designated as auxiliary genes as they are dispensable for viral replication but increase the efficiency of virus transmission in nature (O'Reilly, 1997).

BmNPV *orf11* (*bm11*), a homolog of *Autographa californica* multiple nucleopolyhedrovirus (AcMNPV) *ac19*, is a viral late gene encoding a small protein (Bm11) of 110 amino acids. Bm11 homologues have been shown to constitute DUF1477 baculovirus protein family of unknown function in the NCBI's conserved domain database (Marchlerbauer et al., 2017). The presence of a transmembrane domain or signal peptide could not be predicted through the analysis of Bm11 by TMpred server (Hofmann, 1993) and SignalP 4.1 server (Petersen et al., 2011). Orthologs of Bm11 are found in all GroupIand most Group II alphabaculoviruses, but have not been reported to be encoded by other baculovirus genera. It was previously reported that deletion of Bm11 resulted in the production of infectious virus and therefore *bm11* may be a non essential gene (Ono et al., 2012).

Abbreviations: BmNPV, *Bombyx mori* nucleopolyhedrovirus; OB, occlusion body; BV, budded virus; ODV, occlusion-derived virus; ORF, open reading frame; AcMNPV, *Autographa californica* multiple nucleopolyhedrovirus; *CmR*, chloramphenicol resistance; p.t., post-transfection; p.i., post-infection; *polh*, polyhedrin gene; wt, wild type; MOI, multiplicity of infection; LT_{50}, median lethal time; HearNPV, *Helicoerpa armigera* nucleopolyhedrovirus

* Corresponding author.
E-mail address: wuxiaofeng@zju.edu.cn (X. Wu).

https://doi.org/10.1016/j.virol.2018.10.026
Received 22 August 2018; Received in revised form 26 October 2018; Accepted 29 October 2018
Available online 14 November 2018

To provide a more detailed understanding of the role of *bm11* in the BmNPV infection cycle, we constructed a *bm11*-deletion BmNPV and investigated the function of Bm11 both *in vitro* and *in vivo*. Our data confirmed that Bm11 was not essential for BV production, and we also found that it did not appear to be involved in viral DNA replication. However the *bm11*-deletion mutant decreased the production of OBs and reduced the number of ODVs occluded in polyhedra. The mutant also caused a lengthening of the lethal time of *B. mori* larvae. Furthermore, we examined the subcellular localization of Bm11 and found the protein mainly localized to the intranuclear ring zone at the late stage of infection. Taken together, our results identified *bm11* as an auxiliary gene that affected OB production, ODV occlusion and slowed the pathology of infection.

2. Results

2.1. Bm11 is a conserved and late gene

Orthologs of *bm11* have been identified in all Group I and some group II NPVs (Fig. S1A) (Jehle et al., 2006; Rohrmann, 2014). Alignments of the predicted amino acid sequences showed that the C-terminal region of Bm11 was more conserved than the N-terminal region (Fig. S1B).

To investigate the temporal transcription pattern of *bm11*, total RNA extracted from BmNPV-infected cells at different time points was analyzed by reverse transcriptional (RT)-PCR. The *bm11* transcripts were first detected at 12 h post-infection (p.i.) at a very low level, steadily increased up to 72 h p.i., and remained detectable at 96 h p.i. (Fig. S2A). Next, to determine the *bm11* transcriptional initiation site, 5′ rapid-amplification of cDNA ends (RACE) was performed. Transcription initiation site maps to the second A of the canonical baculovirus late promoter motif ATAAG, which is located 44 nt upstream of the start codon of *bm11* ORF (Fig. S2B). In addition, the precise expression pattern of Bm11 was confirmed by qRT-PCR analysis. As shown in Fig. S2C, the *bm11* transcript was detected at 12 h p.i. and continued to increase up to 48 h p.i.. These results demonstrated that *bm11* was a late gene and is similar to that found for AcMNPV Ac19 (Chen et al., 2013).

2.2. Construction of the bm11 knockout, repair and control BmNPV mutants

To examine the role of *bm11* in the baculovirus life cycle, a BmNPV *bm11*-null mutant bacmid, bBm11KO, was constructed as described previously (Wu et al., 2006). The *bm11* locus was disrupted by introducing a chloramphenicol resistance (*CmR*) gene cassette (Fig. 1) (Wang et al., 2007).

To facilitate observation of viral infection and examine the effect of

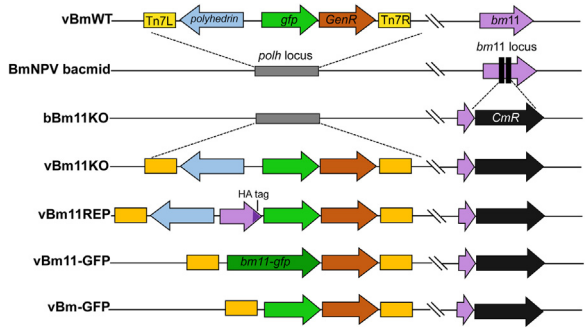

Fig. 1. Schematic diagram of recombinant viruses. A 183 bp of *bm11* in vBm11KO was replaced with a 1100-bp *CmR* cassette. The *bm11* gene under the control of its native promoter and tagged at the C terminus with the HA epitope sequence (black triangle) was inserted at the *polh* locus of the *bm11*-repair virus (vBm11REP). The *bm11-gfp* chimera and GFP alone under the control of the native promoter were inserted into vBm11-GFP and vBm-GFP respectively.

bm11 deletion on OB morphogenesis, the green fluorescent protein-encoding (*gfp)* gene and polyhedrin (*polh)* gene were inserted into the *polh* locus of both vBm11KO and vBmWT (Fig. 1). To confirm that any defective phenotype resulting from the *bm11*-knockout was not due to genomic effects, a *bm11*-repair virus, vBm11REP, was constructed by inserting the *bm11* driven by its native promoter and fused to haemagglutinin (HA) sequence, along with the *gfp* and *polh* genes (Fig. 1).

To further assess the functional role of *bm11* in the viral life cycle, two viruses were constructed to monitor the subcellular localization of Bm11 (Fig. 1). In vBm11-GFP, Bm11 was expressed in-frame with GFP to produce a Bm11-GFP fusion protein under the control of the *bm11* promoter. As a control, GFP alone was expressed under the control of the native promoter in vBm-GFP. All constructs were verified by PCR analysis (data not shown).

2.3. Bm11 exhibits a ring zone distribution during infection

To determine whether the HA-tagged Bm11 was detectable and to establish its temporal expression pattern, an initial time course analysis of Bm11 was performed using vBm11REP. Western blot analysis revealed that Bm11 was initially detected at 24 h p.i. and persisted at 120 h p.i. (Fig. 2A). The result confirmed that *bm11* was a late gene, which is consistent with the transcriptional analyses.

The subcellular localization of the Bm11 protein was analyzed by confocal microscopy (Fig. 2B). At 24 h p.i., Bm11-GFP was observed mainly at the nuclear rim, with a slight distribution in the cytoplasm. Then the fluorescence became condensed along the outer periphery of the nucleus in the BmN cells at 48 h p.i.. By 72 h p.i., a small amount of fluorescence was observed in the center of the nucleus, but Bm11-GFP signal was more concentrated in the intranuclear ring zone. Fluorescence was detected throughout the vBm-GFP-infected cells (Fig. 2B). These observations suggested that Bm11 predominantly exhibited a ring zone distribution at the very late phase of infection.

2.4. Bm11 is not essential for BV production or viral DNA replication

To study the effect of *bm11* deletion on viral proliferation, BmN cells were transfected with vBmWT, vBm11KO or vBm11REP bacmid and observed by fluorescence. At 48 h post-transfection (p.t.), there were no obvious differences in the number of fluorescent cells among these viruses. By 96 h p.t., fluorescence was observed in all three samples (Fig. 3A). When the supernatants from the transfection mixtures were collected at 120 h p.t. and used to infect a second batch of cells, the majority of the infected cells showed successful infection by 96 h p.i., which indicating all three viruses were capable of generating infectious BVs (Fig. 3A).

Viral growth curve assays were conducted to evaluate whether the *bm11* deletion could affect secondary viral infection. BmN cells were infected with each virus and the BV titers were determined by the 50% tissue culture infective dose ($TCID_{50}$) endpoint dilution at given time points. BmN cells infected with each virus revealed a steady increase in BV titer and their growth kinetics were similar (Fig. 3B). qPCR analysis was performed to further detect BV genomes regardless of the construct used. The data from Fig. S3 were in agreement with the $TCID_{50}$ results and both demonstrated that Bm11 is not required for BV production.

qPCR analysis was carried out to analyze the effect of *bm11* deletion on viral DNA replication. BmN cells were transfected with each bacmid. At indicated time points, intracellular viral DNA was extracted and analyzed with the paired primers GP41-F/GP41-R. The results in Fig. 3C showed comparable levels of DNA synthesis for all three constructs, suggesting that Bm11 was not required for DNA replication.

2.5. Bm11 deletion decreases the OB production

Although we found that Bm11 was not essential for BV production and DNA replication, we wanted to determine whether OB production

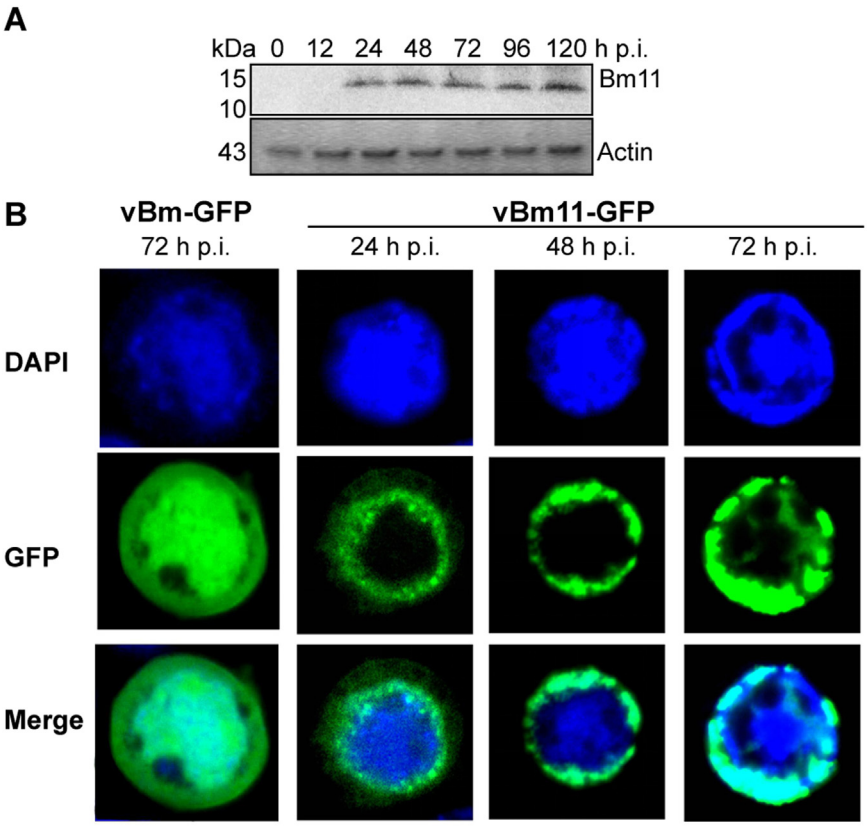

Fig. 2. Temporal expression pattern and subcellular localization of Bm11. (A) Time course analysis of Bm11 expression. BmN cells were infected with vBm11REP at an MOI of 5. The cells were collected at indicated time points. Samples were probed with mouse monoclonal HA antibody to detect Bm11HA. An anti-ACTIN antibody was used as control. Molecular mass standards are shown on the left. (B) BmN cells were infected with vBm-GFP or vBm11-GFP at a MOI of 5. The cells were stained with DAPI for DNA. Confocal fluorescence microscopy was used to examine Bm11 localization (green) at the indicated time points. From left to right: DNA (DAPI; blue), Bm11-GFP (GFP; green) and merged images.

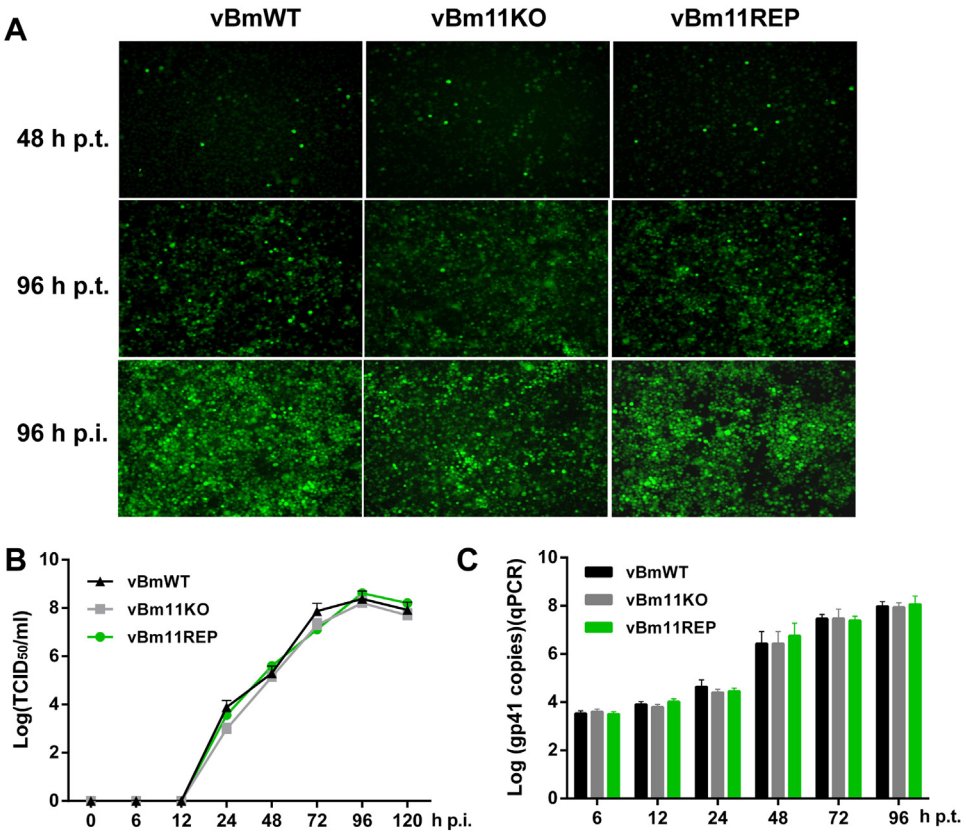

Fig. 3. Analysis of BV production and viral DNA replicationin in BmN cells. (A) Microscopy analysis. Fluorescence microscopy shows the progression of viral infection in BmN cells transfected with vBmWT, vBm11KO and vBm11REP at 48 or 96 h p.t.. (B) Virus growth curve analysis. BmN cells were infected with the three indicated viruses, then the supernatants were harvested at the given time points and quantified for production of infectious BV by $TCID_{50}$ assays. Infectivity was monitored by EGFP expression. (C) Real-time PCR analysis of viral DNA synthesis. At the designated time points, total intracellular DNA was extracted and quantified by qPCR. Each data point was determined by the average of triplicate transfections.

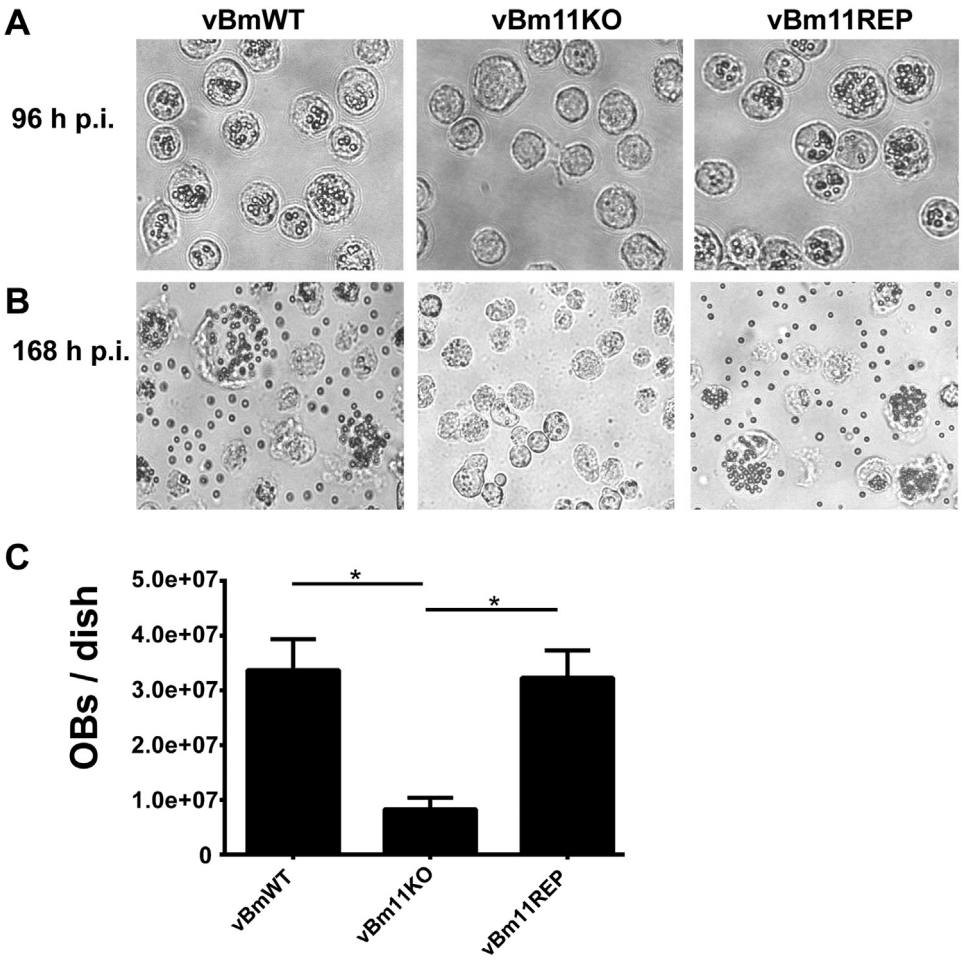

Fig. 4. Analysis of OB production in BmN cells. (A) OB production in BmN cells. Infected cells were observed at 96 h p.i. by light microscopy. (B) Infected cells were observed at 168 h p.i.. (C) Analysis the number of OB in transfected BmN cells. The cells were gently scraped at 168 h p.i. and total OB production was measured using hemocytometer. Data shown are means ± SD ($n = 3$, $P < 0.05$).

in BmN cells was affected. Light microscopy analyses at 96 h p.i. revealed that, whereas OBs were observed in most of the vBmWT or vBm11REP infected cells, the number of OB-containing cells produced from the vBm11KO infection was reduced (Fig. 4A). This suggested that the deletion of *bm11* decreased the OB production but did not prevent the formation of OBs. The infected cells began to lyse by 96 h p.i. and by 168 h p.i., almost all polyhedra were released from the cells (Fig. 4B). To quantify the extent of OB reduction in cells infected with the vBm11KO, we counted the number of released OBs at 168 h p.i.. The OB production was almost comparable in vBmWT or vBm11REP infected cells. However, the intracellular OBs produced by vBm11KO infected cells was only about 25% of the other two samples (Fig. 4C). These results indicated that Bm11 had an important role in OB production.

2.6. Bm11 knockout delays the time of larval death

To examine the effect of *bm11* deletion on larval infection, the BV supernatant from vBm11KO, vBmWT or vBm11REP transfected BmN cells were directly injected into the larvae on the third day of 5th-instar at a dose of 1.0×10^6 $TCID_{50}$ units/larva. The survival curve analyses showed the median lethal times (LT_{50}) of larvae infected with vBm11KO were 24 h longer than the controls (Fig. 5A).

Then, to examine the function of Bm11 on the infectivity of the ODVs, oral infection with 1.0×10^6 OBs was tested on the newly molted silkworm larvae (starved for 24 h). Ingestion of the OBs from the vBm11KO only resulted in a 67% mortality rate even 8 days after feeding. In contrast, the other two viruses resulted in a 100% mortality rate at 7 days (Fig. 5B). Similarly, the LT_{50} of larvae fed with *bm11* deletion virus were also one day longer.

Finally, the infectious BVs released into the hemolymph and the number of OBs was quantified. BV titers of vBm11KO-infected hemolymph produced a comparable amount with vBmWT and vBm11REP (Fig. 5C). As shown in Fig. 5D, significantly fewer OBs were released in vBm11KO-infected larvae. These results were similar to the observation of *in vitro* assays using BmN cells (Fig. 4C).

2.7. Bm11 is not required for the formation of virogenic stroma, ODV or OB

To investigate the reason of delayed larval death caused by vBm11KO in the bio-assays, and to further analyze the effect of *bm11* deletion on virion morphogenesis, electron microscopy analysis was performed. The cells infected with vBmWT displayed typical symptoms of the BmNPV infection at 96 h p.i., such as electron-dense virogenic stroma (VS), nucleocapsid-enveloped ODVs and OBs (Fig. 6A–C) with normal shapes and sizes in the ring zone. In vBm11REP-infected cells, characteristics were similar to those of vBmWT-infected cells (data not shown). Typical symptoms of infection in vBm11KO-infected cells, such as the VS structure and mature enveloped ODVs were also present (Fig. 6E–G). However, the polyhedra from vBm11KO-infected cells appeared to contain fewer ODVs (Fig. 6H) than that of vBmWT (Fig. 6D), although their size and shape were similar, demonstrating that deletion of *bm11* compromised the ODV occlusion.

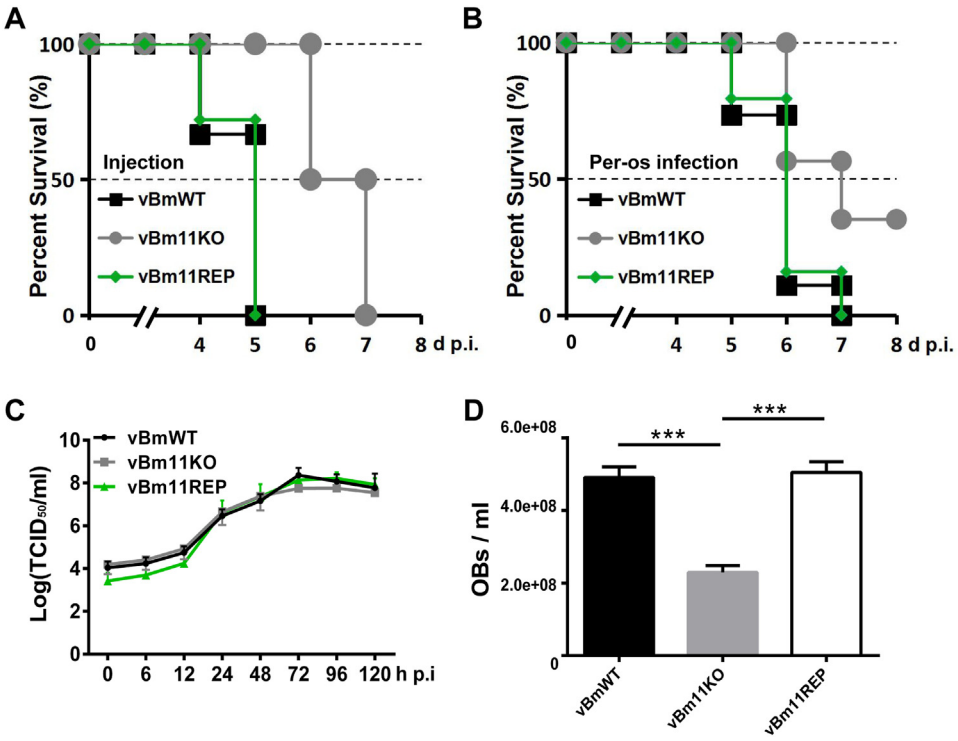

Fig. 5. Analysis of *bm11* deletion on larval infection. (A) For injection, survival curves were from inoculating the BVs into the third day of fifth-instar *B. mori* larvae ($n = 24$). The LT_{50} of vBmWT, vBm11KO and vBm11REP were 5 days, 6 days and 5 days, respectively. (B) For oral infection, newly molted fifth-instar *B. mori* larvaes were fed with 1.0×10^6 OBs ($n = 24$). The LT_{50} of each virus were 6 days, 7 days and 6 days, respectively. The mortality rate of vBm11KO was 67%. Percent survival was by the average of triplicate infections. (C) BV production at 96 h p.i.. The infectious BV titer of larval hemolymph was determined by $TCID_{50}$ assays. (D) OB production. The released OBs in the hemolymph of the infected larvae was collected at 96 h p.i. and counted using hemocytometer. Data shown are means ± SD ($n = 3$, $P < 0.05$).

2.8. The deletion of bm11 affects the embedding of ODV into polyhedra

To further analyze the effect of *bm11* deletion on ODV embedding, we first quantified ODV content by qPCR. For BmNPV, a single nucleocapsid nucleopolyhedrovirus, the DNA copy number presented the ODV number contained in OBs. As shown in Fig. 7A, the ODVs contained in vBm11KO OBs (24.9 ± 1.6 copies/OB) (mean ± SD, $n = 3$) was less than wild type (wt) (34.6 ± 2.3 copies/OB) and repair OBs (33.4 ± 2.2 copies/OB).

Additional TEM observation of polyhedra purified from vBm11KO and vBmWT infected larvae showed significantly fewer ODVs were embedded in OBs due to the *bm11* deletion (Fig. 7B). The number of ODVs was also quantified under the TEM. As shown in Fig. S4, the results indicated similar ODV quantity as described above.

Then we determined the number of ODVs in sections taken from 30 polyhedra of vBmWT and vBm11KO respectively. The number of ODVs from the knockout virus was significantly lower than the wt virus, in which the ODV continued to increase as the diameter of cross-sectional size increased (Fig. 7C).

Finally, the major capsid protein VP39 was used to detect the ODVs. Equal amounts (7.0×10^8) of OBs were dissolved and probed with an antibody recognizing VP39 and anti-POLH antibody for control (Fig. 7D). The analysis revealed that less VP39 was expressed in vBm11KO virus, which also meant the ODV content was reduced. As a control, the expression level of the protein VP39 and POLH in the infected cells were not changed by deleting Bm11 (data not shown). Consistent with the previous analysis, these results showed that the deletion of *bm11* affected the embedding of ODVs into polyhedra,

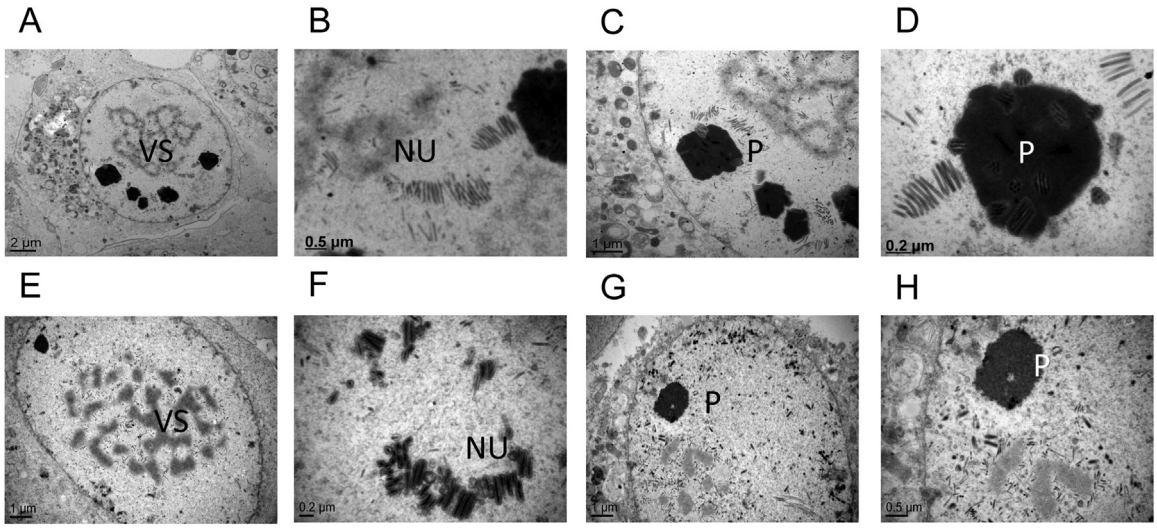

Fig. 6. TEM analysis of BmN cells infected with vBmWT (A–D) or vBm11KO (E-H). (A and E) Electron-dense virogenic stroma (VS). (B and F) Electrondense nucleocapsids aligning with *de novo* developed nuclear envelopes (Nu). (C and D) Polyhedra (P) containing embedded or being-embedded ODVs. (G and H) Polyhedra devoid of embedded virions. Samples were collected at 72 h p.i. for TEM.

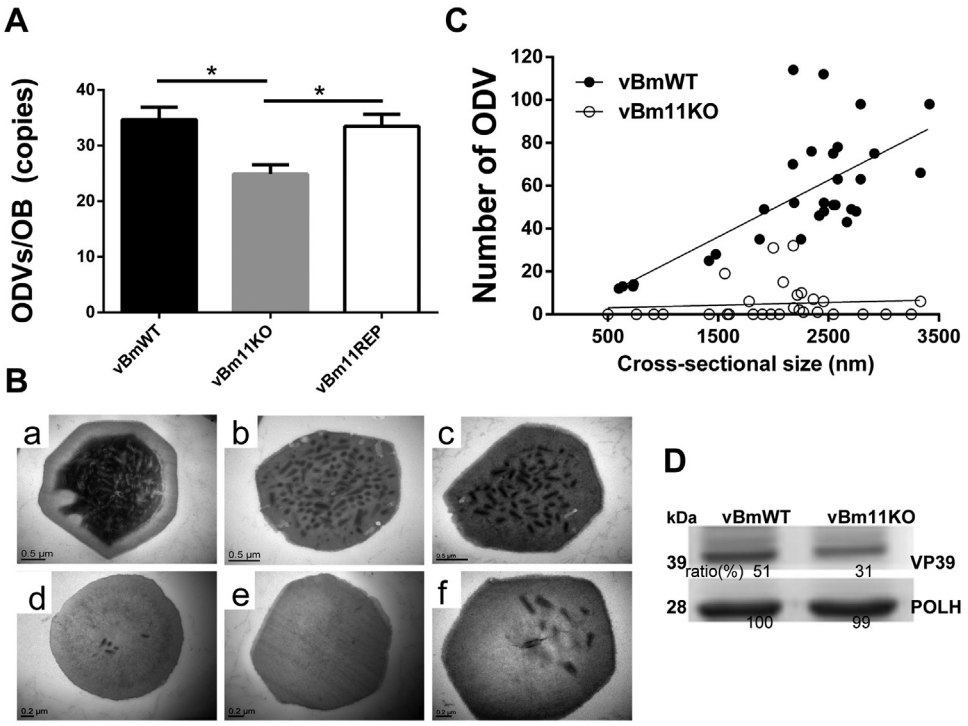

Fig. 7. The comparison of ODV content in OBs from *B. mori* larvae. (A) qPCR analysis of the number of embedded ODV. The viral genome DNA extracted from OBs was used as template. Significant differences were represented as asterisk. (B) TEM analyses of purified occlusion bodies from orally infected larvae. (a–c) occlusion bodies purified from vBmWT are normal shaped with dozens of ODVs inside. (d–f) occlusion bodies purified from vBm11KO infected larvae are mostly with several ODVs inside. Samples were collected at 96 h p.i. for TEM. (C) Correlation between the number of ODV and the cross sectional size of polyhedra. The polyhedron size was measured using Image J software. (D) Western blot analysis of ODV occlusion with the VP39 and POLH antibody. The molecular masses of protein standards are indicated on the left. Relative band intensities are shown at the lower panel.

which might thus reduced the BmNPV oral infection efficiency.

3. Discussion

Bm11 and its homologues are present in all sequenced Group I and some group II NPVs (Rohrmann, 2014), suggesting it may play a vital role in the viral life cycle of these viruses. However, its specific role still remains elusive. In this study, we found that Bm11 was mainly involved in occlusion body production and ODV embedding.

Transcriptional and Western blot analyses revealed that *bm11* was a late gene (Fig. S2 and Fig. 2A), implying that it plays a role at the later stages of viral infection. The subcellular localization of Bm11 revealed that it primarily localized in the intranuclear ring zone during the very late phase of virus infection (Fig. 2B). Previous studies have shown that the virogenic stroma was the active site for virus DNA replication and nucleocapsid assembly (Fraser, 1986), and the ring zone for ODV assembly and the formation of occlusion bodies (Williams and Faulkner, 1997). Therefore, the location of Bm11 in the ring zone, rather than in VS implied that its functions might be involved in the ODV embedding and OB production.

The electron microscopy analyses demonstrated that the knockout did not affect nucleocapsid assembly at the VS (Fig. 6E and F), indicating that the new viral DNA could be incorporated into capsids. This is in accordance with qPCR analysis which revealed that Bm11 was not required for viral DNA replication (Fig. 3C). In addition, the formation of virus-induced intracellular microvesicle, mature ODV and polyhedra were not affected in the knockout virus.

The present study revealed that occlusion body production was compromised by the knockout of *bm11* (Figs. 4 and 5D). Many genes have been reported to be key factors for OB production. For example, the analysis of *bm8* and *bm71* found their deletion decreased the OB production in the middle silk glands and blood of insects, respectively (Zhang et al., 2012). The deletion of the *fp* gene *(bm49)* was reported to not only decreased OB yield but also caused an increased BV production (Katsuma et al., 2006). The analysis of Pp31 *(*Yamagishi et al., 2007*)* and Bm5 (Kokusho et al., 2016) showed that the reduced production was due to a lower expression of *polh* gene. These results suggested that the reduced level of OB production might be caused by the transcriptional down-regulation of the polyhedron-associated genes, which were required for the efficient polyhedrin expression.

Our results have confirmed a previous report (Ono et al., 2012) that showed that the knockout of *bm11* had no impact on infectious BV production in cell culture (Fig. 3A and B). However we found that using larval bio-assays that Bm11 was involved in efficient viral infection *in vivo* by direct injection (Fig. 5A). Similar negative effects were observed in early studies of Bm33 (Katsuma et al., 2008), Bm34 (Katsuma and Shimada, 2009) and Bm56 (Xu et al., 2008). Neither the *bm33*, *bm34, bm56* nor *bm11* was essential for BV production *in vitro,* but the deletion of any one lowered the BV infectivity *in vivo*. Therefore, the LT_{50} of baculovirus were influenced by multiple genes, and the specific mechanism is still unclear.

The TEM observations found that the deletion of *bm11* resulted in a remarkable effect on OBs with fewer ODVs (Fig. 6). This was consistent with the qPCR and Western blotting analysis, which showed a decrease in the average amount of DNA per OB and reduced amounts of VP39 in *bm11* deleted BmNPV mutants (Fig. 7A and D) respectively. As shown in Fig. 7C, there were more ODVs in the cross section diameter of polyhedra from the wt virus suggesting that Bm11 might facilitate ODV occlusion. These results suggested that the decreased infectivity in *B. mori* larvae infected with equal amount OBs (Fig. 5B) were due to the reduction of ODVs embedded into the polyhedra.

So far, sixteen proteins and their homologues from AcMNPV, *Helicoerpa armigera* nucleopolyhedrovirus (HearNPV) or BmNPV have been reported to be associated with ODV embedding. Many of these genes were shown to interfere with the envelopment of nucleocapsids to become ODV, some were shown to be required for the formation of intranuclear microvesicles and subsequent mature ODV occlusion, whereas deletion of others led to a defect in nucleocapsid assembly. Moreover, Ha72 (Huang et al., 2014), Bm64 (Chen et al., 2015) (both are Ac78 homologues) and Ac114 (Wei et al., 2012), which were all associated with BV and ODV, were found to have an impact on the enveloped ODV embedding. The deletion of *ha83 (*Yu et al., 2015*)*, as one of the 20 unique genes of HearNPV, resulted in larger occlusion bodies of cubic shape containing a reduced quantity of DNA. As for P26 (Ac136), (Wang et al., 2009) suggested it might act in concert with P10 and P74 to regulate the virion occlusion process. According to the

above analyses, these all differed from our observations of the *bm11* knockout. Therefore, we suggest the hypothesis that *bm11* deletion affects the process of ODV occlusion in an indirect way such as affecting efficient nucleocapsid envelopment, reducing ODV production or interrupting the expression of some ODV occlusion-related genes. In fact, ODV morphogenesis is a complex process requiring the coordination of various factors, and any interference of these factors will disrupt the virion envelopment and subsequent occlusion. Additional studies will need to be carried out to uncover the mechanism underlying the ODV occlusion.

In conclusion, our study demonstrated that *bm11* was a multifunctional auxiliary gene that was not essential for BV production and mature ODV formation, but did affect OB production and ODV embedding into polyhedra.

4. Materials and methods

4.1. Virus, cell line and insects

The *Escherichia coli* strains BW25113 containing BmNPV genome and pKD46, and BW25141 harboring plasmid pKD3 were kindly provided by Mary Berlyn (Yale university, USA). The *E. coli* strain DH10H containing a helper plasmid pMON7124 was preserved by our laboratory. BmN cells were cultured at 27 °C in Sf-900 II SFM supplemented with 10% FBS from Gibco (Life Technologies). Titers of BV were determined by a $TCID_{50}$ endpoint dilution assay in BmN cells in triplicate (Yu et al., 2015). The fifth-instar *B. mori* larvae were reared at 25 ℃.

4.2. RT-PCR, 5′ RACE and qRT-PCR analysis

BmN cells (2.5×10^6 cells/35-mm plate) were infected with BmNPV at a multiplicity of infection (MOI) of 5 $TCID_{50}$/cell and harvested at selected time points. The total RNA was prepared using the RNAiso Reagent (TaKaRa). First-strand DNA complementary to the mRNA (cDNA) were synthesized with 1 μg total RNA and oligo (dT) primers using PrimeScript™ 1st Strand cDNA Synthesis Kit (TaKaRa). Then the cDNA mixtures were amplified using *bm11*-specific primers (Table. S1) to detect the *bm11* transcripts. BmNPV *ie-1* gene and *actin* gene were used as the control.

The 5′ RACE procedure was performed using the Smarter RACE cDNA Amplification kit (Clontech) employing 1 μg purified total RNA isolated from BmNPV infected cells at 48 h p.i.. The first strand cDNA was synthesized with a *bm11*-specific primer Bm11-RACE primer according to the manufacturer's instructions. The PCR products were gel purified and cloned into the pMD19-T (TaKaRa) for sequencing.

qPCR was performed to confirm the transcription pattern of Bm11 as previously described (Kokusho et al., 2016). The qPCR was performed using the 7300 Real-Time PCR system (ABI, USA) under the following conditions: 95 °C for 30 s and 40 cycles of 95 °C for 5 s and 60 °C for 31 s (Chen et al., 2015).

4.3. Construction of recombinant BmNPVs with disrupted bm11

The *bm11*-knockout BmNPV bacmid, in which the *bm11* gene was disrupted by inserting a *CmR* cassette for antibiotic selection, was generated though λ-Red recombinant system as previously described (Yang et al., 2016). The fragment of *CmR* gene was amplified using primers Bm11KO-F and Bm11KO-R from pKD3. The two primers contained 68 and 65 bp sequences homologous to the upstream and downstream flanking regions of *bm11*, respectively; a stop codon was also introduced. The *CmR* fragment was gel purified and electroporated into *E.coli* BW25113 cells to obtain bBm11KO. The insertion was confirmed by PCR analysis with three different primers. The identified bBm11KO was extracted and electro-transformed into *E.coli* DH10H to generate DH10Bm11KO cells containing both the *bm11*-knockout bacmid and the helper plasmid.

In order to determine if *bm11* deletion has any effect on virus infection and occlusion body morphogenesis, the *bm11* knockout, the repair and the wt BmNPV bacmids were constructed as previously described (Yang et al., 2016). The pFB1-PH-GFP donor plasmid was constructed by inserting *polh* and *gfp* genes under the *polh* promoter and *ie1* promoter, respectively (Xu et al., 2008). The pFB1-PH-GFP was transformed into electrocompetent DH10Bm11KO or DH10BmBac cells to generate the vBm11KO bacmid or the vBmWT bacmid, respectively.

To construct repair virus, a 737 bp fragment containing *bm11* gene with its native promoter region and a C-terminal HA sequence was amplified from BmNPV genome using primers Bm11Re-F and Bm11Re-R. The PCR product was digested with *Eco*RI/*Xba*I and cloned into pFB1-PH-GFP (Yang et al., 2009) to generate the repair donor plasmid. Electrocompetent DH10B cells containing bBm11KO and the pMON7124 helper plasmid were transformed with the donor plasmid to generate the vBm11REP bacmid. The recombination products were confirmed by PCR with M13 forward and reverse primers.

To monitor the localization of Bm11 in BmNPV infected BmN cells, GFP was fused at the C-terminus of Bm11 under the control of the *bm11* promoter to create a Bm11-GFP fusion protein. A recombinant fusion bacmid for vBm11-GFP were constructed as previously described (Chen et al., 2015). The *bm11* with its native promoter was PCR-amplified with the primers Bm11sub-F and Bm11sub-R and the *gfp* gene was amplified using the primers EGFP-F and EGFP-R.

4.4. Time course analysis of Bm11 expression

In order to establish the temporal expression pattern of Bm11, BmN cells were infected with vBm11REP as previously described. The infected cell lysates were collected at various time points and boiled in 1 × sodium dodecyl sulfate (SDS) loading buffer for 10 min. Samples were electrophoresed on SDS polyacrylamide gel electrophoresis (SDS-PAGE) and Western blotting with a primary antibody mouse monoclonal anti-HA (1:2000, Abcam) and then incubated with secondary antibodies, Goat-anti mouse (1:5000, Sigma). The blots were detected by Beyc ECL (Beyotime).

4.5. Subcellular localization analysis of Bm11 during infection

Immunofluorescence assays were performed as described previously with minor modification (Chen et al., 2015). BmN cells were infected with vBm11-GFP or vBm-GFP at an MOI of 5 in triplicate. At various time points, the supernatant was removed and the cells were fixed in 4% paraformaldehyde with PBS for 20 min, washed 3 times and permeabilized in 1% bovine serum albumin (BSA) for 30 min. Prior to analysis, the cells were subsequently stained with DAPI (Beyotime) at 1 μg/ml for 15 min. Finally images were captured using the Zeiss LSM 780 confocal laser scanning microscope and processed with Zen lite measuring software (Carl Zeiss).

4.6. Analysis of BV propagation from cells and larvae

To analyze infectious BVs production, the viral growth curve analysis was performed as previously described (Chen et al., 2015). Specifically, BmN cells (2.0×10^6 cells/35-mm plate) were infected with recombinant viruses. This point was defined as 0 h p.i. At the designated time points, the progression of viral infection was monitored by fluorescence microscopy and the virus supernatants were collected at the same time (Chen et al., 2015). The $TCID_{50}$ was determined on BmN cells in 96-well plates, and analyzed by fluorescent microscopy after infection for 5 days in triplicate (Reed and Muench, 1938; Summers and Smith, 1987).

qPCR was performed to confirm the baculovirus stocks as previously described (Lo and Chao, 2004). 250 μl supernatant from each infection mixture was processed by viral DNA kit (Omega, USA). Purified DNA sample was mixed with SYBR® Premix ExTaq (TaKaRa, Japan) and the

qPCR primer targeting a 100-bp region of the BmNPV *gp41* gene.

For larval infection, fifth-instar larvae were placed on the ice and injected of 10 μl of viral suspension (1.0×10^6 $TCID_{50}$ units/larva), then returned to fresh mulberry leaves at 25. At 96 h p.i., the hemolymph of infected larvae was collected, hemolymph BV titer was determined by plaque assay on BmN cells (Kokusho et al., 2016).

4.7. Quantitative analysis of viral DNA synthesis

qPCR analysis was performed to assess viral DNA synthesis as previously described (Chen et al., 2012). The intracellular total DNA was extracted with the EasyPure Genomic DNA Kit (TransGen). The qPCR was performed described previously.

4.8. OB production in BmN cells and in B. mori larvae

For OB production, BmNPV-transfected BmN cells were gently scraped at 168 h p.i. and total OB production was observed under light microscopy and calculated as described previously for three times. For larval infection, the hemolymph of infected larvae was collected at 96 h p.i. and the released OBs were counted using a hemocytometer as described previously (Kokusho et al., 2016).

4.9. Transmission electron microscopy

BmN cells (2.5×10^6 cells) were infected with vBm11KO or vBmWT at an MOI of 5. At 72 h p.i., the cells were collected and fixed with 2% glutaraldehyde in PBS. Then the samples were embedded in epoxy resin, sectioned at 70 nm, stained with uranyl acetate and lead citrate, as described previously (Katsuma and Kokusho, 2017). The blocks were viewed under a Hitachi Model SU8010 transmission electron microscope (TEM) operating at 80 kV.

To analyze the content of ODV embedded in OB of vBm11KO and vBmWT, 1.0×10^8 purified OBs from infected fifth-instar *B.mori* larvae were treated and viewed by TEM as mentioned above.

4.10. B. mori larvae bio-assay

Bio-assays were conducted using a leaf disc feeding assay to inoculate 5th instar larvae (Erlandson et al., 2007). OB suspensions collected from vBm11KO, vBmWT or vBm11REP in various concentrations were applied to the leaf discs. After 30 min drying period, a cohort of 24 larvae was used for each treatment, and each assay was repeated in triplicate. Mortality was recorded every 12 h until all larvae pupated or 8 days post-treatment. Survival curves were analyzed using GraphPad Prism6 software.

4.11. Quantification of ODVs released from larvae

At first, ODVs were purified from infected fifth-instar *B. mori* larvae as described previously (Peng et al., 2010, 2012). 7×10^8 OBs of vBm11KO and vBmWT were treated with 6 ml DAS solution for 10 min 37 °C, then the solution was neutralized with 1 ml 0.5 M Tris-HCl (pH 7.5) and incubated for 2 min. The supernatant was collected by centrifugation at 4000 rpm for 2 min and ODVs were pelleted by centrifugation at 15,000 rpm for 25 min at 4 °C.

To detect the content of embedded ODV released from infected larvae fed with different virus type, the expression level of VP39 and POLH were analyzed by SDS-PAGE and Western blot analysis with the anti-VP39 and anti-POLH antibody separately (Kokusho et al., 2016).

In addition, the number of embedded ODV in different samples can be obtained through the copy number of genomic DNA. The viral genome DNA extracted from 1.0×10^6 polyhedron was used as template (Yu et al., 2015). qPCR was performed with *gp41* quantitative primers according to the method described.

Acknowledgments

We deeply thank Professor George Rohrmann for his critical reading and suggestions on this manuscript.

AUTHOR STATEMENTS

This work was funded by the National Natural Science Foundation of China (project 31772675 and 31472146). We declare that there is no conflict of interest for our study. All the experiments involving animals were conducted in strict accordance with the Institutional Animal Care and Use Committee of Zhejiang University.

Appendix A. Supporting information

Supplementary data associated with this article can be found in the online version at doi:10.1016/j.virol.2018.10.026.

References

Braunagel, S.C., Summers, M.D., 1994. Autographa californica nuclear polyhedrosis virus, PDV, and ECV viral envelopes and nucleocapsids: structural proteins, antigens, lipid and fatty acid profiles. Virology 202, 315–328.
Braunagel, S.C., Summers, M.D., 2007. Molecular biology of the baculovirus occlusion-derived virus envelope. Curr. Drug Targets 8.
Chen, L., Hu, X., Xiang, X., Yu, S., Yang, R., Wu, X., 2012. Autographa californica multiple nucleopolyhedrovirus odv-e25 (Ac94) is required for budded virus infectivity and occlusion-derived virus formation. Arch. Virol. 157, 617–625.
Chen, L., Shen, Y., Yang, R., Wu, X., Hu, W., Shen, G., 2015. Bombyx mori nucleopolyhedrovirus (BmNPV) Bm64 is required for BV production and per os infection. Virol. J. 12, 1–11.
Chen, Y.R., Zhong, S., Fei, Z., Hashimoto, Y., Xiang, J.Z., Zhang, S., Blissard, G.W., 2013. The transcriptome of the baculovirus Autographa californica multiple nucleopolyhedrovirus in Trichoplusia ni cells. J. Virol. 87, 6391–6405.
Erlandson, M., Newhouse, S., Moore, K., Janmaat, A., Myers, J., Theilmann, D., 2007. Characterization of baculovirus isolates from Trichoplusia ni populations from vegetable greenhouses. Biol. Control 41, 256–263.
Federici, B.A., 1997. Baculovirus Pathog. 33–59.
Fraser, M.J., 1986. Ultrastructural observations of virion maturation in Autographa californica nuclear polyhedrosis virus infected Spodoptera frugiperda cell cultures ☆. J. Ultrastruct. Mol. Struct. Res. 95, 189–195.
Granados, R.R., Lawler, K.A., 1981. In vivo pathway of Autographa californica baculovirus invasion and infection. Virology 108, 297–308.
Herniou, E.A., Olszewski, J.A., Cory, J.S., O'Reilly, D.R., 2003. The genome sequence and evolution of baculoviruses. Annu. Rev. Entomol. 48, 211–234.
Hofmann, K., 1993. TMBASE-A database of membrane spanning protein segments. Biol. Chem. Hoppe-Seyler 374, 1–3.
Huang, H., Wang, M., Deng, F., Hou, D., Arif, B.M., Wang, H., Hu, Z., 2014. The ha72 core gene of baculovirus is essential for budded virus production and occlusion-derived virus embedding, and amino acid K22 plays an important role in its function. J. Virol. 88, 705–709.
Jehle, J.A., Blissard, G.W., Bonning, B.C., Cory, J.S., Herniou, E.A., Rohrmann, G.F., Theilmann, D.A., Thiem, S.M., Vlak, J.M., 2006. On the classification and nomenclature of baculoviruses: a proposal for revision. Arch. Virol. 151, 1257–1266.
Katsuma, S., Fujii, T., Kawaoka, S., Shimada, T., 2008. Bombyx mori nucleopolyhedrovirus SNF2 global transactivator homologue (Bm33) enhances viral pathogenicity in B. mori larvae. J. Gen. Virol. 89, 3039–3046.
Katsuma, S., Horie, S., Daimon, T., Iwanaga, M., Shimada, T., 2006. In vivo and in vitro analyses of a Bombyx mori nucleopolyhedrovirus mutant lacking functional vfgf. Virology 355, 62–70.
Katsuma, S., Kang, W., Shini, T., Ohishi, K., Kadota, K., Kohara, Y., Shimada, T., 2011. Mass identification of transcriptional units expressed from the Bombyx mori nucleopolyhedrovirus genome. J. General. Virol. 92, 200.
Katsuma, S., Kokusho, R., 2017. A conserved glycine residue is required for proper functioning of a baculovirus VP39 protein. J. Virol. 91 (6).
Katsuma, S., Shimada, T., 2009. Bombyx mori nucleopolyhedrovirus ORF34 is required for efficient transcription of late and very late genes. Virology 392, 230–237.
Keddie, B.A., Aponte, G.W., Volkman, L.E., 1989. The pathway of infection of Autographa californica nuclear polyhedrosis virus in an insect host. Science 243, 1728.
Kokusho, R., Koh, Y., Fujimoto, M., Shimada, T., Katsuma, S., 2016. Bombyx mori nucleopolyhedrovirus BM5 protein regulates progeny virus production and viral gene expression. Virology 498, 240–249.
Lo, H.R., Chao, Y.C., 2004. Rapid titer determination of baculovirus by quantitative real-time polymerase chain reaction. Biotechnol. Progress. 20, 354–360.
Marchlerbauer, A., Bo, Y., Han, L., He, J., Lanczycki, C.J., Lu, S., Chitsaz, F., Derbyshire, M.K., Geer, R.C., Gonzales, N.R., 2017. CDD/SPARCLE: functional classification of proteins via subfamily domain architectures. Nucleic Acids Res. 45, D200–D203.
Miao, X.X., Xub, S.J., Li, M.H., Li, M.W., Huang, J.H., Dai, F.Y., Marino, S.W., Mills, D.R., Zeng, P., Mita, K., 2005. Simple sequence repeat-based consensus linkage map of Bombyx mori. Proc. Natl. Acad. Sci. USA 102, 16303.

O'Reilly, D.R., 1997. Auxiliary Genes of Baculoviruses. Springer, US.
Ono, C., Kamagata, T., Taka, H., Sahara, K., Asano, S., Bando, H., 2012. Phenotypic grouping of 141 BmNPVs lacking viral gene sequences. Virus Res. 165, 197–206.
Peng, K., Lent, J.W.M.V., Boeren, S., Fang, M., Theilmann, D.A., Erlandson, M.A., Vlak, J.M., Oers, M.M.V., 2012. Characterization of novel components of the baculovirus per Os infectivity factor complex. J. Virol. 86, 4981–4988.
Peng, K., van Oers, M.M., Hu, Z., van Lent, J.W., Vlak, J.M., 2010. Baculovirus per os infectivity factors form a complex on the surface of occlusion-derived virus. J. Virol. 84, 9497.
Petersen, T.N., Brunak, S., Heijne, G.V., Nielsen, H., 2011. SignalP 4.0: discriminating signal peptides from transmembrane regions. Nat. Methods 8, 785–786.
Reed, L.J., Muench, H., 1938. A simple method OF estimating fifty per cent endpoints. Am. J. Hyg. 27.
Rohrmann, G.F., 2014. Baculovirus Molecular Biology, 3rd edition. .
Slack, J., Arif, B.M., 2006. The baculoviruses occlusion-derived virus: Virion structure and function. Adv. Virus Res. 69, 99–165.
Summers, M.D., Smith, G.E., 1987. A manual of methods for baculovirus vectors and insect cell culture procedures. Bull. B - Tex. Agric. Exp. Station (USA) 40, 1–56.
van Oers, M.M., Vlak, J.M., 2007. Baculovirus genomics. Curr. Drug Targets 8,.
Wang, L., Salem, T.Z., Campbell, D.J., Turney, C.M., Kumar, C.M., Cheng, X.W., 2009. Characterization of a virion occlusion-defective Autographa californica multiple nucleopolyhedrovirus mutant lacking thep26, p10 and p74 genes. J. General. Virol. 90, 1641–1648.
Wang, Y., Wu, W., Li, Z., Yuan, M., Feng, G., Yu, Q., Yang, K., Pang, Y., 2007. ac18 is not essential for the propagation of Autographa californica multiple nucleopolyhedrovirus. Virology 367, 71–81.
Wei, W., Zhou, Y., Lei, C., Sun, X., 2012. Autographa californica multiple nucleopolyhedrovirus orf114 is not essential for virus replication in vitro, but its knockout reduces per os infectivity in vivo. Virus Genes 45, 360–369.
Williams, G.V., Faulkner, P., 1997. Cytological Changes and Viral Morphogenesis During Baculovirus Infection. Springer, US.
Wu, W., Lin, T., Pan, L., Yu, M., Li, Z., Pang, Y., Yang, K., 2006. Autographa californica multiple nucleopolyhedrovirus nucleocapsid assembly is interrupted upon deletion of the 38K gene. J. Virol. 80, 11475–11485.
Xu, H.J., Yang, Z.N., Zhao, J.F., Tian, C.H., Ge, J.Q., Tang, X.D., Bao, Y.Y., Zhang, C.X., 2008. Bombyx mori nucleopolyhedrovirus ORF56 encodes an occlusion-derived virus protein and is not essential for budded virus production. J. General. Virol. 89, 1212.
Yamagishi, J., Burnett, E.D., Harwood, S.H., Blissard, G.W., 2007. The AcMNPV pp31 gene is not essential for productive AcMNPV replication or late gene transcription but appears to increase levels of most viral transcripts. Virology 365, 34–47.
Yang, R., Zhang, J., Feng, M., Wu, X., 2016. Identification of Bombyx mori nucleopolyhedrovirus bm58a as an auxiliary gene and its requirement for cell lysis and larval liquefaction. J. Gen. Virol. 97, 3039–3050.
Yang, Z.N., Xu, H.J., Thiem, S.M., Xu, Y.P., Ge, J.Q., Tang, X.D., Tian, C.H., Zhang, C.X., 2009. Bombyx mori nucleopolyhedrovirus ORF9 is a gene involved in the budded virus production and infectivity. J. General. Virol. 90, 162.
Yu, H., Xu, J., Liu, Q., Liu, T.X., Wang, D., 2015. Ha83, a chitin binding domain encoding gene, is important to Helicoverpa armigera nucleopolyhedrovirus budded virus production and occlusion body assembling. Sci. Rep. 5, 11088.
Zhang, M.J., Cheng, R.L., Lou, Y.H., Ye, W.L., Zhang, T., Fan, X.Y., Fan, H.W., Zhang, C.X., 2012. Disruption of Bombyx mori nucleopolyhedrovirus ORF71 (Bm71) results in inefficient budded virus production and decreased virulence in host larvae. Virus Genes 45, 161–168.